Examining Reception of GNSS Underwater using a Smartphone

Matthew Yuan, *Columbia University*, Sherman Lo, *Stanford University*

BIOGRAPHIES

Matthew Yuan is a freshman at Columbia University. He conducted this research while a high school student in St. Paul's Academy High School in Concord, New Hampshire as part of their Applied Science & Engineering Program (ASEP) 2020

Sherman Lo is a senior research engineer at the Stanford GPS Laboratory. He received his Ph.D. in Aeronautics and Astronautics from Stanford University in 2002. He has and continues to work on navigation robustness and safety, often supporting the FAA. He has conducted research on Loran, alternative navigation, SBAS, ARAIM, GNSS for railways and automobile. He also works on spoof and interference mitigation for navigation. He has published over 100 research papers and articles. He was awarded the ION Early Achievement Award.

ABSTRACT

One of the limits of GNSS is in its use in the oceans and other bodies of water. While it can serve some ocean surface applications, its use for tracking marine life that rarely surfaces is limited. However, if we can understand how far underwater GNSS may be received, we can further extend its use envelope and perhaps enable it to serve more marine tracking applications. This paper examines the limits of GNSS reception underwater with measurements data from a smartphone as well as theoretical modeling. Different types of water (tap, distilled and salt) are examined as they have different electrical properties which affects the attenuation of the GNSS signals. The paper also examines the difference in smartphones L1 and L5 reception both on land and underwater.

I. INTRODUCTION

When we think of GNSS applications, we naturally think of applications such as mapping, car navigation or location-based apps such as Uber as these are some of the most common ways we interact with GNSS. Other applications that come to mind may be aircraft and unmanned aerial vehicle (UAV) navigation, precision timing, and robotic farming. A commonality with these applications is that none of them are water based, even though many of today's devices that hold a GNSS receiver, such as a smart phone or smart watch, can operate in water. Indeed there is a lack of use of GNSS in water environments even though it can operate under a little water, as when people use their smartwatch GPS while swimming. Operating underwater could be another important application area for GNSS. We have no other positioning tool that is as precise, ubiquitous, globally-available and low costs (< $1 for a smartphone GNSS module in bulk). If we can devise ways of using it in challenging marine applications, it can be of great benefit to marine science, conservation, and monitoring of ocean borne equipment. For example, we can learn a lot more about the precise habits of sea life or we can make sure fishing nets and other equipment do not get lost and entangle wildlife, etc. If the animal or equipment being monitored typically stays on the water surface, using GNSS should be relatively straight-forward. What is more challenging is for creatures that do not come up often or only surfaces for brief periods of time (i.e. a few seconds). This is challenging for GNSS as unassisted GNSS, which is likely the case for tracking in the oceans, takes typically 30 or more seconds to develop a position solution. While we can improve the speed to a few seconds with various assisted GNSS (A-GNSS) techniques [1] or post processing [2][3], obtaining GNSS positions in a few seconds without real time assistance is difficult.

Hence, in this paper, we examine how deep we can operate GNSS in different water types to understand how we may be able to extend the operating window of GNSS in water. Empirical measurements are made with a smartphone and compared to previously developed theoretical models. Examination of different factors such as water type (tap, distilled and saline) and frequency (L1 and L5) is conducted.

II. BACKGROUND

Tracking Marine Targets with GNSS

Tracking water borne creatures and maritime equipment has become increasingly common place and desirable. While most tracking is done without GNSS, such as with pop up satellite archival tags (PSATs) [4], these technologies are not nearly as precise as GNSS (kilometers or 10's of kilometers). Being able to get accurate positions in the marine environment opens up a host of possible applications and science. As the need to monitor, protect, and understand the oceans become increasingly important, we need to develop ways to provide GNSS based tracking suitable for various marine applications. One example application is the tracking marine gear such as fishing lines and crustacean traps (i.e. crab and lobster pots). When such gear is lost, at a minimum they become flotsam and jetsam polluting the oceans. This can harm wildlife as the equipment can tangle up a whale or other marine creatures preventing their nature movements such as surfacing to breathe. Knowing precise location can allow for their efficient retrieval. This is valuable both for saving the equipment for reuse and for saving marine life. GNSS can also be useful for tracking the increasing number of autonomous underwater vehicles (AUV) such as wave gliders. Also, GNSS provides a level of accuracy that can be used for marine science and wild life protection. Precise knowledge of marine life location at particular times can help determine habits and also identify potential poachers.

Figure 1. Tracking marine animals with GPS. Sea turtle (left) from turtlewatch.info and seal (Lars Boehme, University of St. Andrews)

The limitation with GNSS use in water is that the receiver/antenna typically needs to be above water to operate. GNSS use is relatively straight-forward for use for applications where the GNSS device is attached to animals or equipment with constant or regular long duration stays above the water surface. For example, lobster pots are attached by rope to a buoy that stays above surface. However even in this case, the trap buoy may be dragged under if something, such as a whale, gets entangled in its rope. Extending marine utility and handling different scenarios means that developing GNSS with the ability to operate with only intermittent and brief periods above water. Some technologies have been developed to extend GNSS use in water by requiring only a brief period of GNSS visibility. One technique as used in systems such as FastLoc capture 10s of milliseconds radiofrequency GNSS samples for post processing [2]. This only require very brief observation and external source of ephemeris. More importantly, it requires a bespoke GNSS receiver which makes the tag costly compared to a tag that uses consumer off the shelf (COTS) or mass market GNSS chipsets. Some COTS chipsets can use techniques based on A-GNSS concepts and can gather the requisite information with only a few seconds of GNSS reception. Such technology extends the use of GNSS in water for some applications such as tracking sea turtles or pinnipeds such as sea lions as seen in Figure 1 [5] and opens up more possibilities for GNSS use in water. But there are many other creatures that comes to the surface much more briefly whose tracking or monitoring valuable for scientific and conservation purposes. Anyone who has experienced whale watching, see Figure 2, and been disappointed by the brief glimpses of whales as they quickly come up to the surface for their breaths then dive down understand the brevity of the time window of the creature on the surface. The second or two that they are on the surface may not be sufficient for GNSS to develop position information if there is no real time assistance to provide it information on satellites visible and help narrow its acquisition search space. However, if we can operate under a little bit of water, in other words, start and end operations a few seconds earlier and later, respectively, to

extend that window, we would have enough time to get some acquisition information. This would allow for tracking of those animals or equipment bobbing in the water. This is the purpose of our study.

In this work we examine GNSS performance underwater two ways: In the next section, we discuss the empirical tests of GNSS underwater. In the section after that, we delve into prior art modeling of attenuation of GNSS signals in water. Finally, we compare the results from the two methods.

Figure 2. Whales and other creature may only be on the surface for a few seconds (source NOAA)

III. EMPIRICAL ANALYSIS OF GNSS UNDERWATER

Field Test Design & Set Up

Empirical measurements were taken in the field using a smartphone which was immersed in a container of the target medium at a specified depth. The smartphone used was the Xiaomi Mi 8, shown in Figure 3, which uses the Broadcom BCM47755 GNSS module. This was the first smartphone, introduced 2018, with two frequency GNSS (L1 and L5). It is also a global phone so Beidou and Galileo can be received in addition to GPS and GLONASS. For the test, GNSS was operated in stand-alone mode (i.e. without assistance data to aid reception to enhance reception). This is partly done so that we can be sure that the effects seen are due purely to GNSS and not to other network enhancements. It is also done because remote tags generally do not have assistance information that can improve sensitivity. Android GNSS raw measurements tools and the Google app, GNSSLogger, was used to collect the data [6]. The data collection was done by running sets of trials which each trial involving submerging the phone in a waterproof bag in water inside a large plastic container at specified depths - 0, 1, 2.5, and 10 centimeters (cm). The overall set up is shown in Figure 4. The container with depth marked every cm is shown in Figure 5. The main tests were conducted in San Francisco near Rincon Park and Pier 40, shown in Figure 6. These are locations that are reasonably unobstructed by buildings on the east side since they are on the San Francisco bay.

Figure 3. Xiaomi Mi8, first dual frequency smartphone using Broadcom BCM47755 (souce: xiaomi)

A total of six sets of trials were conducted – two for each of the three different types of water were used: 1) tap, 2) distilled, and 3) salt water. Salt water was obtained from the San Francisco bay near where the trials were conducted. For each media (tap, distilled and salt water), we conduct 2 sets of trials. Each set consisted of trials at water depths of 0, 1, 2.5, and 10 cm with 0 cm being a dry measurement to provide our reference value. A trial at each depth lasted about five minutes allowing for the receiver to settle to a steady state and providing enough data to make a reasonable average. After the trials, the data was collected from the smartphone and processed. The measurements were filtered so that only satellites whose line of sight (LOS) do not get near buildings are used. This filtering was done based on the satellite azimuth and elevation, our data collection location, and a 3-D map. This minimizes attenuation due to factors other than the submerging media (e.g. buildings and multipath) so that the data more accurately reflects attenuation due to water. Identification of potentially obstructed signals was done using Google earth 3-D building maps and knowledge of satellite azimuth and elevations at the time of data collection. For the latter, Trimble's online GNSS planning tool, gnssplanning.com, was used. We then calculate the average signal to noise density, known as the C/No, for satellites on each frequency and at each depth. To calculate attenuation from water, the average C/No at depth was differenced with the average C/No out of water (i.e. 0 cm depth).

Figure 4. Equipment for data collection in the field; q-tips used as stand offs to keep the smartphone off the bottom of the plastic container

Figure 5. Test container and waterproof bag for smartphone GNSS underwater experiment on Pier 40

Figure 6. Test Locations: Rincon Park (upper star), Pier 40 (lower star, inset photo)

Test Data Processing

The raw data is processed so as to minimize changes to C/No due to factors other than being in water so we can calculate the reception changes due to water only. One important step is to get C/No from unobstructed satellites. To do that, we process the GNSSLogger text file in Matlab. We use satellite visibility information to determine relative azimuth and elevation. We then use Google Earth to determine if those directions are near buildings and filter out using any satellites near buildings in our calculations. This is done to try to minimize building effects as we only want to measure water effects. The filtering out metric was conservative and eliminated many satellites. The filtering tools are shown in Figure 7. Filtering out these signals also tends to eliminate satellites at low elevation. This has the additional benefit of eliminating satellite signals that would come in from the side of the container rather than the top. We also measure automatic gain control (AGC) results as this available on the GNSS raw measurements from the Mi 8. In the analysis in this paper, we solely used the AGC values assure that the data sets did not have degradation due to interference.

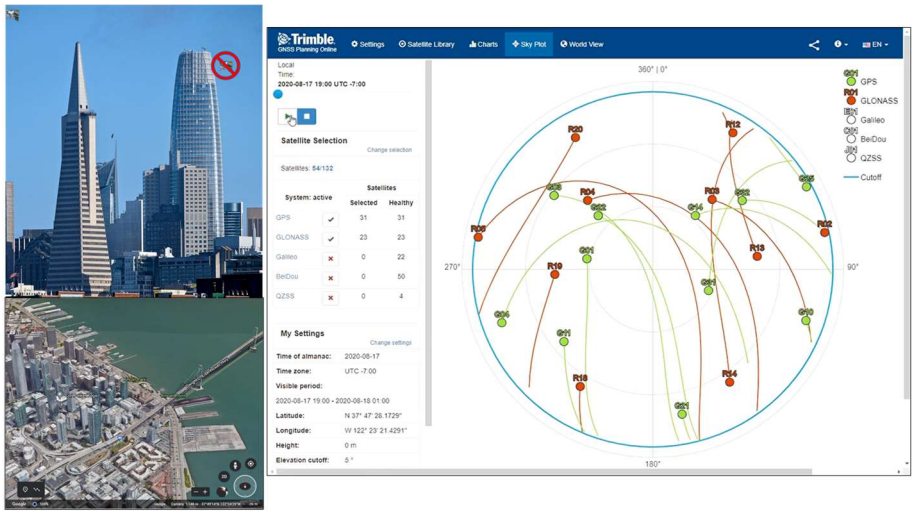

Figure 7. Using Google Earth and Trimble GNSS Planning Tool to Eliminate Questionable Satellites

Statistics are then generated for each accepted satellite then entered in a excel spreadsheet. For each satellite we get about 300 sec (5 min) of data for depth (it may be NaN if tracking is lost). For each depth and satellite, we find the mean C/No. For the analysis in this paper, we use the depth of water rather than calculate the distance in water from the individual LOS. For signals coming in from the top this means that true path in water will be slightly lower than the depth of water due to the geometry. For signals coming in from the side, which should be fewer as we eliminate many low elevation satellite, this distance can be greater or less than the depth of water as there is a few centimeters of water between the phone to the air/water interface on each side. The mean (average) was done on the C/No value in decibel Hertz (dB-Hz) and hence it is a geometric average in power. From the statistics, we can get a plot C/No vs depth for each satellite. An example is shown in Figure 8. Figure 9 shows the C/No over time for several PRNs for one trial. Finally, Figure 10 shows C/No results for different PRN averaged at each depth for L1 (circle) and L5 (diamond). This plot only shows satellites that have both L1 and L5 signals, with the same color used for a given PRN, so that we can compare the effect of frequency. One observation is that for each satellite, the C/No is higher for L1 than L5 at the surface (0 depth) but this trend reverses under water. The better on land performance of L1 in a smartphone, despite L5 having 3 dB more power, has been seen by other groups.

.

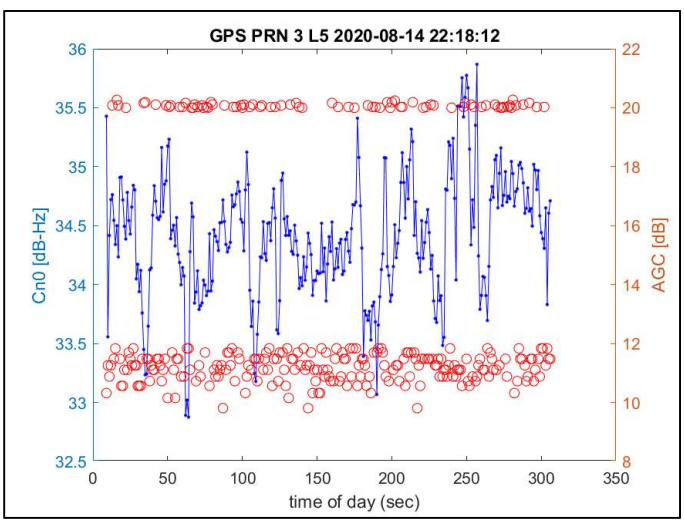

Figure 8. GPS PRN C/No and L1 AGC data for one underwater trial

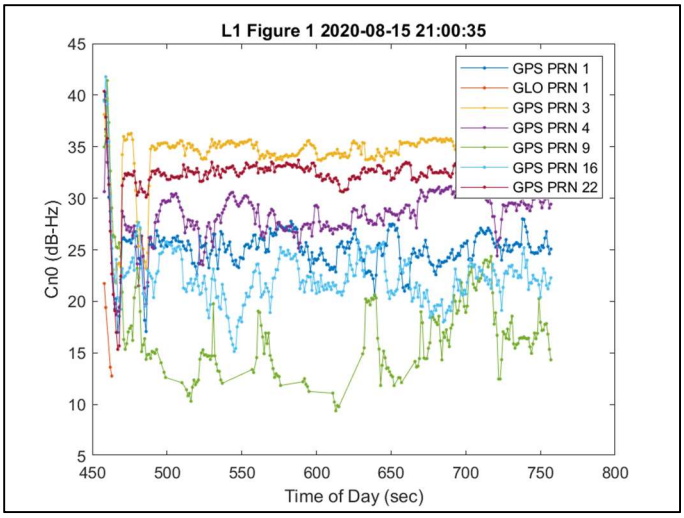

Figure 9. GPS C/No for various satellite for one test trial

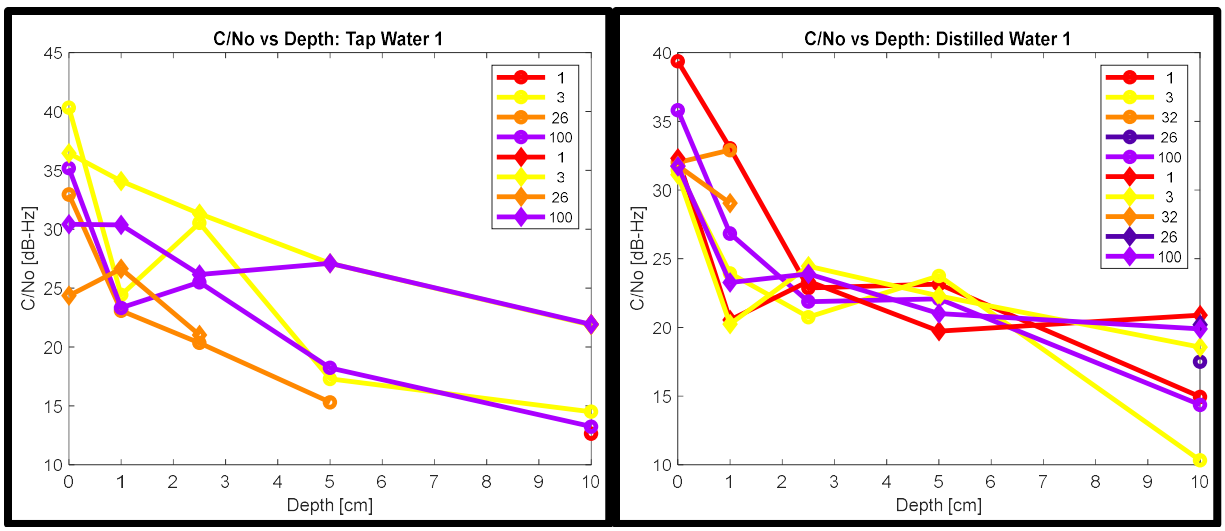

Figure 10. Average C/No of Water (Tap - left, Distilled - right) at Various Depths for L1 (circle) and L5 (diamond) for 4 different PRN

MODELING OF GNSS UNDERWATER

The empirical results are compared to models have been developed for estimating the attenuation of radio frequency (RF) signals as the signal transitions from air (or vacuum) to another media such as water. The comparison is done by examining the attenuation that we measured with attenuation calculated from existing models. The attenuation models are derived from several sources and compared with results from those models. This section rederives the models to examine attenuation at GNSS frequencies (and our targeted depths) which is generally not shown in the plots and results of the references. Additionally, our analysis work found some errors and inconsistencies which necessitated re-deriving the model.

Basic Forms of Attenuation

The attenuation is divided into two components: transmission and propagation loss. This is seen in Figure 11. Transmission loss is loss due to the signal passing from one medium (e.g. air) to another (e.g. water). Propagation loss is loss due to the movement of the signal through the new media and is distance dependent. These losses depend on many factors including the electromagnetic properties such as the permittivity, conductivity and permeability of the media. So, these losses will depend on the media. As these properties are different for distilled water, fresh water and salt water, we examined two models – one for fresh water and one for salt water.

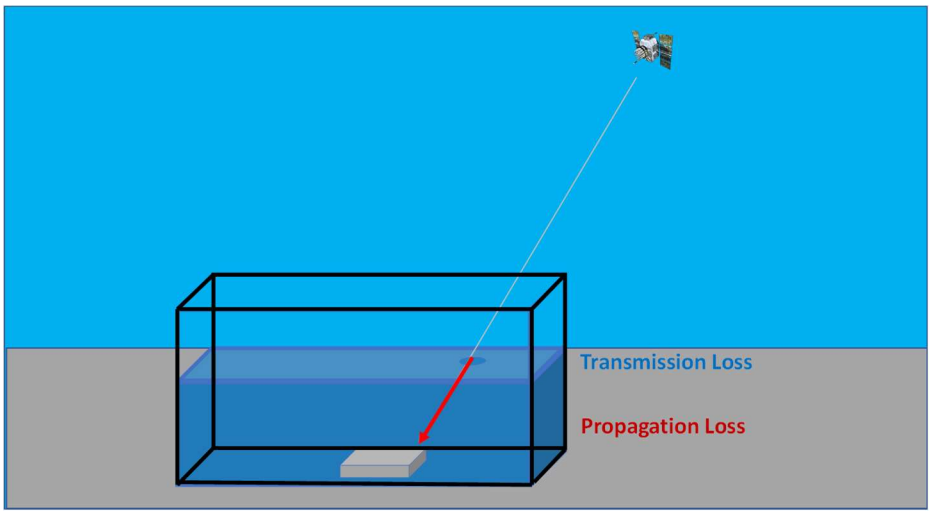

Figure 11. Forms of attenuation as a signal enters underwater

Derivation of Models suing Prior Art

We analyzed prior art to model attenuation in fresh [7] and salt [8][9] water and reproduced their results. Reproduction is necessary as the figures in the relevant works generally are not shown out to GNSS frequencies. Additionally, it helps us understand and derive the findings. This validation is needed as we also found errors in some of the published works.

Starting with propagation loss, a key variable affecting this attenuation is permittivity. Both the fresh and salt water models ([7],[8], [9]) are based on the Debye relaxation model for the permittivity of a medium as a function of frequency. Equation (1) shows the Debye model for the relative permittivity, ε_r, from [7][9] where f and ω are the linear and angular frequency of our signal, f_{rel} and ω_{rel} are the linear and angular relaxation frequency of the media, and ε_{rs} and $\varepsilon_{r\infty}$ are the relative permittivity of the media at zero and the relaxation frequency, respectively. σ is the conductivity of the medium. And despite the different looking formulations in the two papers, we rederived them and showed that they are essentially the same model with different assumption due to the different media (fresh vs salt water) examined. Indeed, the seawater model equation from [8] can be shown to be the same as Equation (1) above but with a flipped sign on the imaginary part. This did not change our result. We use $\varepsilon_{r\infty}$= 4.9 as indicated in [8][9] though reference [7] used a value of 4.22. Hence the Equation (1) formulation applies to both fresh and salt water with different parameter values which are generally empirically derived. [7] presents these parameter values for freshwater which is mostly derived from [11] though with some mistakes. An important parameter is conductivity which is modeled in [9] and reproduced in [8], though with some transcription errors. This is most useful for salty (saline) water. The saltwater parameter models from [9], shown in Equations (2)-(4), depend on temperature and salinity. For freshwater, we used σ= 0.01 Siemens (S)/m where S is the inverse of ohm. For saline water, the value varies to up to 8. Generically for salt water σ=4 is used but [9] provides an empirically based model, shown in Equations (3)-(6), that is a function of temperature and practical salinity unit (PSU). We use the model with temperature and salinity values of 25 C and 35 PSU, respectively.

$$\varepsilon_r = \varepsilon_{r\infty} + \left[\frac{\varepsilon_{rs}-\varepsilon_{r\infty}}{1+\left(i\frac{f}{f_{rel}}\right)}\right] - \frac{i\sigma}{2\pi f \varepsilon_0} \qquad (1)$$

$$\sigma_{25C}(S_{sw}) = S_{sw}(0.18252 - 1.4619\cdot 10^{-3}S_{sw} + 2.093\cdot 10^{-5}S_{sw}^2 - 1.282\cdot 10^{-7}S_{sw}^3) \quad (2)$$

$$\varphi = \Delta[2.033\cdot 10^{-2} + 1.266\cdot 10^{-4}\Delta + 2.464\cdot 10^{-6}\Delta^2 - S_{sw}(1.849\cdot 10^{-5} - 2.551\cdot 10^{-7}\Delta + 2.551\cdot 10^{-8}\Delta^2)] \quad (3)$$

$$\Delta = (25 - T) \qquad (5)$$

$$\sigma(T, S_{sw}) = \sigma_{25}\ (S_{sw})e^{-\varphi} \qquad (4)$$

With these models, we can calculate the propagation attenuation factor which is given in Equation (5) as can be seen in reference [7][9][10]. The permittivity, ε, is the product of the relative permittivity ε_r of water from the Debye model with the permittivity of vacuum ε_0. Again, this is calculated with the conductivity, σ, and signal frequency, f, or angular frequency, $\omega = 2\pi f$. Finally, the propagation loss in dB can be calculated for a given distance with its formulation shown in Equation (6).

$$\alpha_r = \omega\sqrt{\mu\varepsilon}\left\{\frac{1}{2}\left[\sqrt{1+\left(\frac{\sigma}{\omega\varepsilon}\right)^2}\right]-1\right\}^{\frac{1}{2}} \qquad (5)$$

$$\alpha_p = 10 * log_{10}(e^{-2\alpha_r d}) \qquad (6)$$

Next, we examine the transmission loss. The transmission loss depends on whether the signal enters with normal or oblique incidence. For this discussion we assume normal incidence though we model both types of incidences. Equation (7) presents the equation for the loss in dB where * signifies the complex conjugate. This depends on T_c, transmission coefficient, which in turn depends on the intrinsic impedance, η_1, as shown in Equation (8). In [7], the intrinsic impedance is given by Equation (9) whereas in [9], it is given by Equation (10). This makes sense as the conductivity of fresh water is low at 0.1 S/m compared to that of seawater and Equation (9) reduces to Equation (10) for zero conductivity.

$$\alpha_t = 10 * log_{10}\left(|T_c|^2 Re\left(\frac{\eta_0}{\eta_1^*}\right)\right) \qquad (7)$$

$$T_c = \frac{2\eta_1}{\eta_0+\eta_1} \qquad (8)$$

$$\eta_1 = \sqrt{\frac{i\omega\mu_1}{\sigma+i\omega\varepsilon_r\varepsilon_0}} \qquad (9)$$

$$\eta_1 = \sqrt{\frac{\mu_1}{\varepsilon_r\varepsilon_0}} \qquad (10)$$

Reference [9] (referred to by [8] but with typos) provides detailed empirical models for calculating the relaxation time constant, the inverse to the relaxation (angular) frequency, as a function of temperature and salinity. For the sake of brevity, interested readers are asked to refer to those references for the models - we use the model with temperature and salinity values of 25 C and 35 PSU.

For oblique incidence, we can use much of the previous derivation. Using Snell's law, we can relate θ_t with θ_i, where θ_i is the angle of incidence and θ_t is the angle of transmission, by Equation (11). In Equation (11) $\bar{\varepsilon_r}$ is the relative permittivity between the two media. It equals to the index of refraction of the transmission medium (medium being entered) divided by the index of refraction of the initial medium squared – this is shown in Equation (12). From calculating the angle of transmission, we can calculate the transmission coefficient as shown in Equations (13) and (14) which provides the loss given the signal polarization - parallel or perpendicular, respectively. This is then used to calculate the transmission loss as shown in Equation (15) which shows the transmission loss for a signal with parallel polarization. Having the angle of transmission also allow us to calculate the propagation loss for signals with parallel and perpendicular polarization. These are equal and shown in Equation (16). These results are found in [7].

$$\cos\theta_t = \sqrt{1-\sin^2\theta_i/\bar{\varepsilon_r}} \qquad (11)$$

$$\bar{\varepsilon_r} = \left(\frac{\eta_1}{\eta_0}\right)^2 \qquad (12)$$

$$T_{c,\parallel} = \frac{2\eta_1\cos\theta_i}{\eta_0\cos\theta_i+\eta_1\cos\theta_t} \qquad (13)$$

$$T_{c,\perp} = \frac{2\eta_1\cos\theta_i}{\eta_0\cos\theta_t+\eta_1\cos\theta_i} \qquad (14)$$

$$\alpha_{t,\parallel} = 10 * log_{10}\left(\left|T_{c,\parallel}\right|^2 Re\left(\frac{\eta_0}{\eta_1^*}\right)\right) \qquad (15)$$

$$\alpha_{p,\parallel} = \alpha_{p,\perp} = 10 * log_{10}\left(e^{-2\alpha_r d/\cos\theta_t}\right) \qquad (16)$$

Comparison with Prior Art

Figure 12 presents plots from two of the references discussed above. Note they do not go out to GNSS frequency or do they have the fine resolution at the depths that we care about. With GNSS, we can only tolerate about 20 dB of loss so examining 100 dB or more of loss is well beyond our interest area. In comparison, Figure 13 shows corresponding plots that we generated from rederiving their models. Note that they do not perfectly match though they do match for the most part on a gross level. The one major exception is the increase in total loss in fresh water for frequencies beyond 10 MHz. This could not be replicated from our derivation and implementation of their model. Nor could we find anything in their derivations that would suggest that increase. Given the errors or discrepancies that we found, we cannot tell if it is an issue of our derivation, some issue with their implementation or if they forgot to add a term.

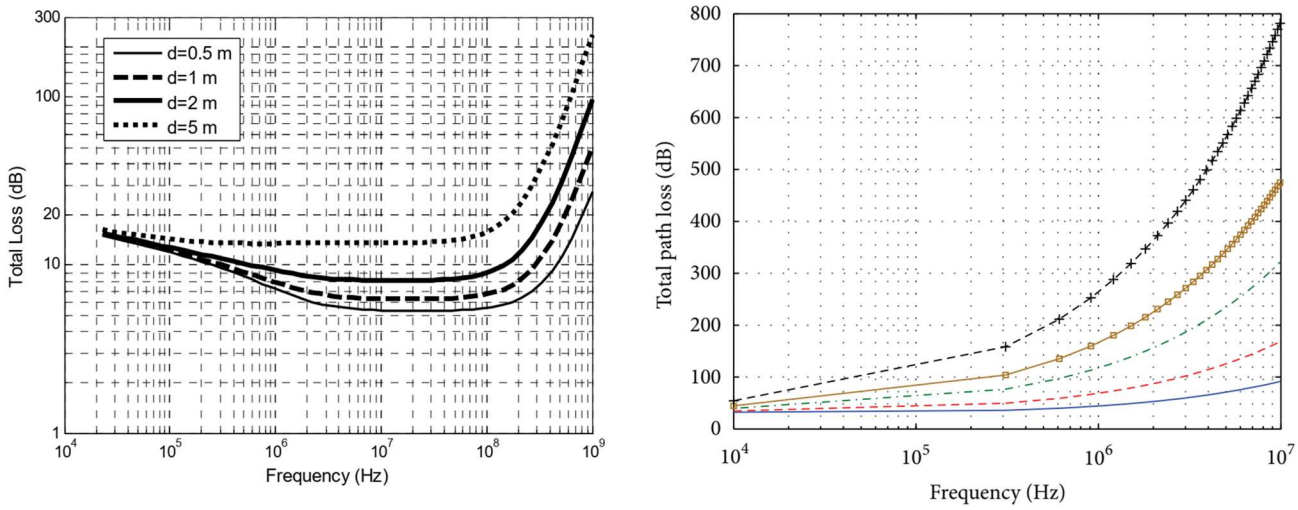

Figure 12. Total attenuation for fresh water (left, [7] at normal incidence) and salt water (right, [8])

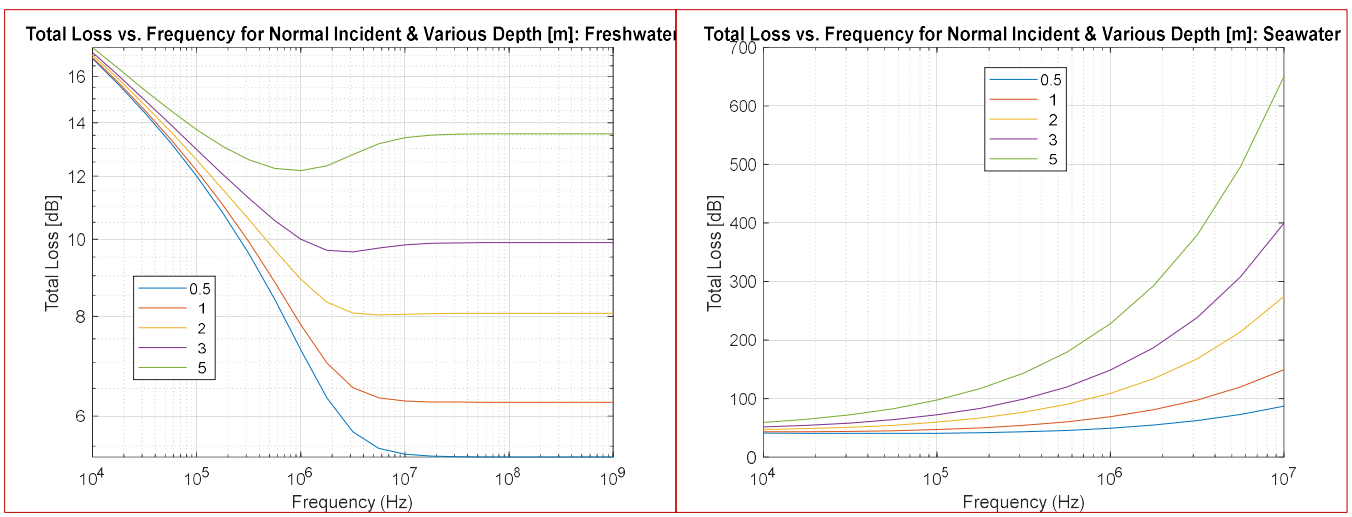

Figure 13. Derived theoretical models for total loss (attenuation) at different frequencies and depths (in meters) under fresh (left) and salt/sea (right) water

RESULTS & COMPARISON

Empirical and Theoretical Attenuation

Several useful insights come from this work which will help inform future design and use of GNSS in maritime environment. The important finding for our work is that GNSS can be reasonably received: 1) in fresh water to about a depth of 10 cm or a little bit more and 2) in salt water only to a depth of about 2.5 cm due to its greater attenuation. While better antennas and GNSS processing may improve the reception depth, the incremental increased depth for salt water may be only a few centimeters given the attenuation gradient with depth. Overall, we found the empirical results roughly follow previously developed models. The correspondence between the empirical measurement and model is approximate with the deviation between them differing depending for the freshwater and saltwater comparison. Finally, while our empirical results found that L5 performance in air was worse than L1 and this trend reversed in water, the attenuation models do not suggest such a change. This indicate this effect must be the result of another factor.

The empirical results from freshwater (either distilled or tap) showed greater loss than expected based on modeling, particularly on L1. The L1 freshwater comparisons are shown in Figure 14 and Figure 16. These plots show a roughly a 5-10 dB bias which may be due to the unmodeled interface (the plastic container or silicon bag that contained the smartphone) or the smartphone itself. Performance in freshwater at L5 is shown in Figure 15 and Figure 17. We see that the bias is less and the measured data more closely hew to the model. L5 empirical result showed less attenuation overall compared to L1. This is expected due to its lower frequency. This can be seen when comparing Figure 14 to Figure 15 or Figure 16 to Figure 17.

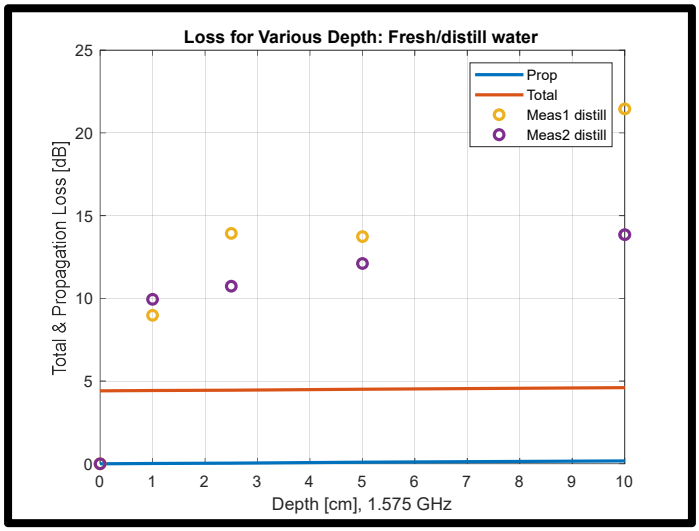

Figure 14. Total and Propagation Path Loss of GPS L1 (1575.42 MHz) C/N0 at Various Depths of Distilled Freshwater. Experimental total loss (2 sets of trials: yellow and purple circles) were calculated for C/N0 data taken under 0, 1, 2.5, 5, & 10 cm depths of bottled distilled water. The blue line represents propagation loss theoretical model, while the orange line shows theoretical model of total path loss.

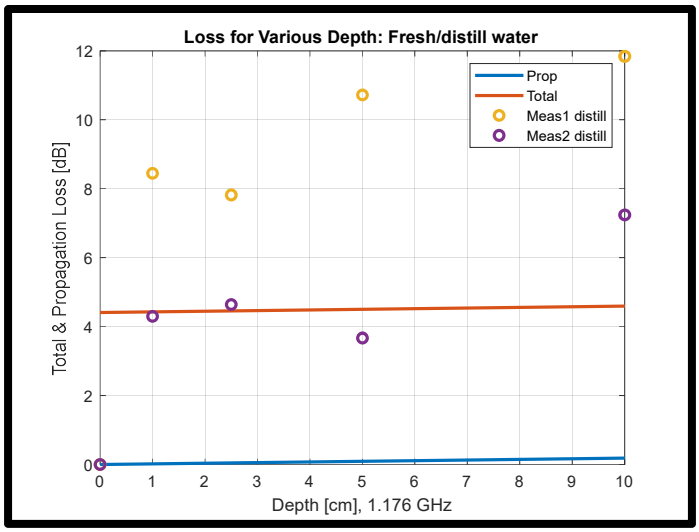

Figure 15. Total and Propagation Path Loss of GPS L5 (1176.45 MHz) C/N0 at Various Depths of Distilled Freshwater. Experimental total loss (2 sets of trials: yellow and purple circles) were calculated for C/N0 data taken under 0, 1, 2.5, 5, & 10 cm depths of bottled distilled water. The blue line represents propagation loss theoretical model, while the orange line shows theoretical model of total path loss.

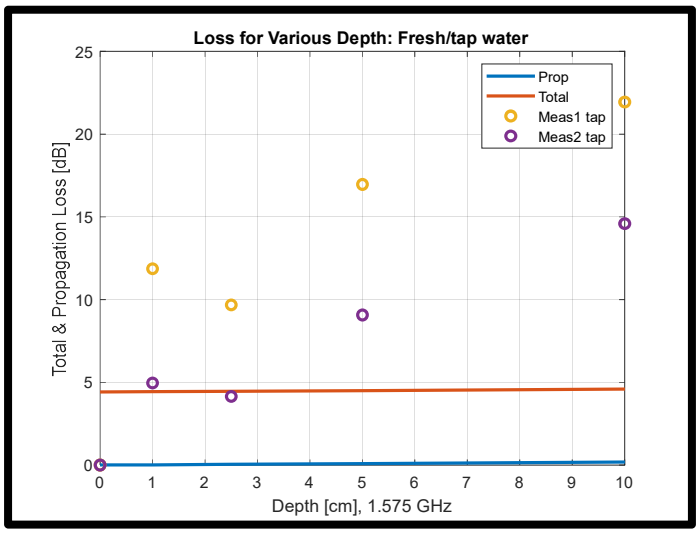

Figure 16. Total and Propagation Path Loss of GPS L1 (1575.42 MHz) C/N0 at Various Depths of Tap Freshwater. Experimental total loss (2 sets of trials: yellow and purple circles) were calculated for C/N0 data taken under 0, 1, 2.5, 5, & 10 cm depths of running tap freshwater. The blue line represents propagation loss theoretical model, while the orange line shows theoretical model of total path loss.

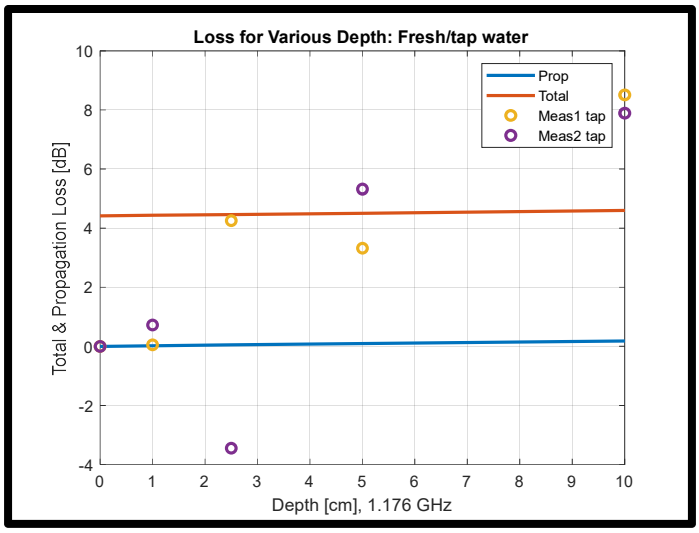

Figure 17. Total and Propagation Path Loss of GPS L5 (1176.45 MHz) C/N0 at Various Depths of Tap Freshwater. Experimental total loss (2 sets of trials: yellow and purple circles) were calculated for C/N0 data taken under 0, 1, 2.5, 5, & 10 cm depths of running tap freshwater. The blue line represents propagation loss theoretical model, while orange line shows theoretical model of total path loss.

Attenuation in salt water is significantly greater than for fresh water as shown in Figure 18 and Figure 19 for L1 and L5, respectively. As seen in the figures, the empirical data well matches the model attenuation for propagation loss only. Again, this difference may be partly attributable to not modeling the more complex interface of the experiment. Also, there are not a lot of data points at different depths to compare to the model due to the rapid attenuation. The attenuation was such that GNSS signals were not received at 10 cm in all cases. Figure 18 shows that in L1 the attenuation is about 20 dB with a depth of 2.5 cm. This is roughly the attenuation experienced on L1 in freshwater at our maximum test depth of 10 cm. Figure 19 shows that on L5, there were no available measurements at 2.5 cm and lower. This means that the signals were so attenuated by that depth that the receiver was not able to track the signals. While the expectation from the freshwater results is that L5 should be slightly less effected, this is not seen in the measurements. The reason for this may be two factors: 1) fewer available L5 signals and 2) weaker reception of L5 signals by the smartphone (which will be discussed later). While all GPS satellites transmit on L1, only about half of GPS satellites transmit on L5. After we eliminate satellites that may be affected by buildings, we are usually left with a few (< 4) L5 signals. If one or two signals are loss, then we may lose L5 completely whereas we could lose many more L1 signals and still have a measurement.

An unanticipated second observation is that the L5 is generally weaker than L1 by about 8-10 dB when out of water. This result is something mentioned to us by a principal from Google Android location which he attributed to limited room for antenna in the smartphone which results in fitting in an antenna that is too small for L5 due to its longer wavelength (than L1). This would result in greater reception inefficiency for L5 and hence lower received power. This difference is not as evident under water. Part of this may be attributed to the lower attenuation at lower frequencies though the models show it to be very minimal (< 1 dB for freshwater at our depths). But it may also be due to index of refraction of water which reduces the speed of the signal and hence reduces the wavelength of the signal. If this is the case, it suggests that some of the experimentally found losses may be due to antenna inefficiencies which is not something we modeled or considered. This is an important point if we design a rapid GNSS tag for use underwater, especially if it uses other GNSS frequencies.

Figure 20, which presents the results from Figure 10 but only showing the curve for the average C/No of satellites with measured signals on L1 and L5, shows this difference more clearly. While the difference is more evident in tap water, it is still clear that L5 is better than L1 in distilled water.

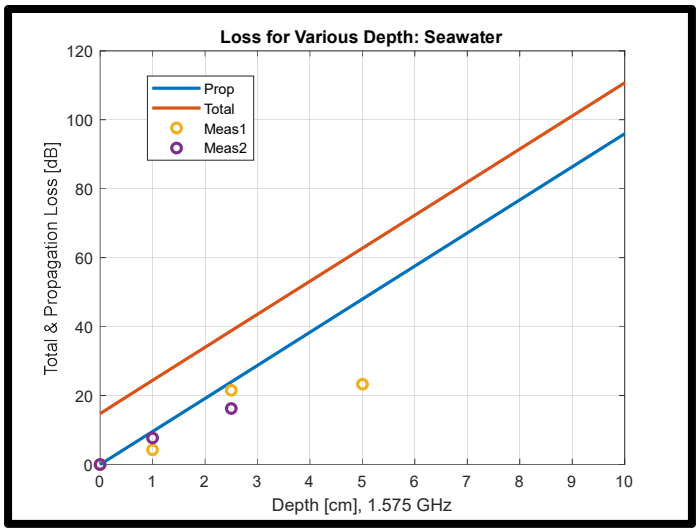

Figure 18. Total and Propagation Path Loss of GPS L1 (1575.42 MHz) C/N0 at Various Depths of Seawater. Experimental total loss (2 sets of trials: yellow and purple circles) were calculated for C/N0 data taken under 0, 1, 2.5, 5, & 10 cm depths of San Francisco Bay seawater. The blue line represents propagation loss theoretical model, while the orange line shows theoretical model of total path loss.

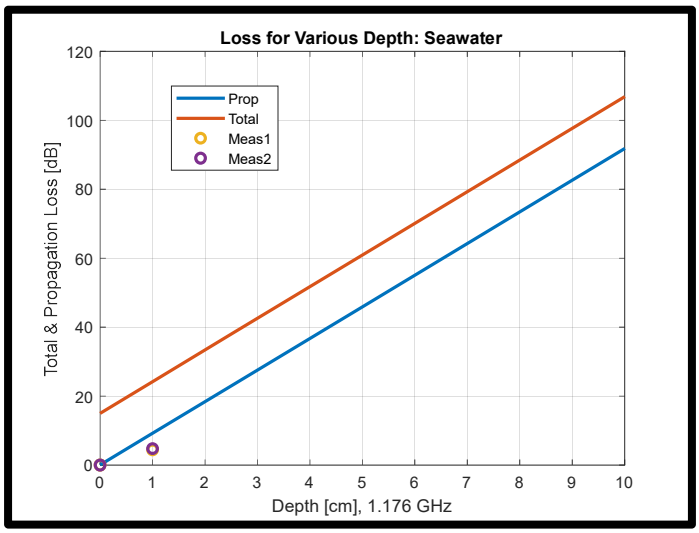

Figure 19. Total and Propagation Path Loss of GPS L5 (1176.45 MHz) C/N0 at Various Depths of Seawater. Experimental total loss (2 sets of trials: yellow and purple circles) were calculated for C/N0 data taken under 0, 1, 2.5, 5, & 10 cm depths of San Francisco Bay seawater. The blue line represents propagation loss theoretical model, while the orange line shows theoretical model of total path loss.

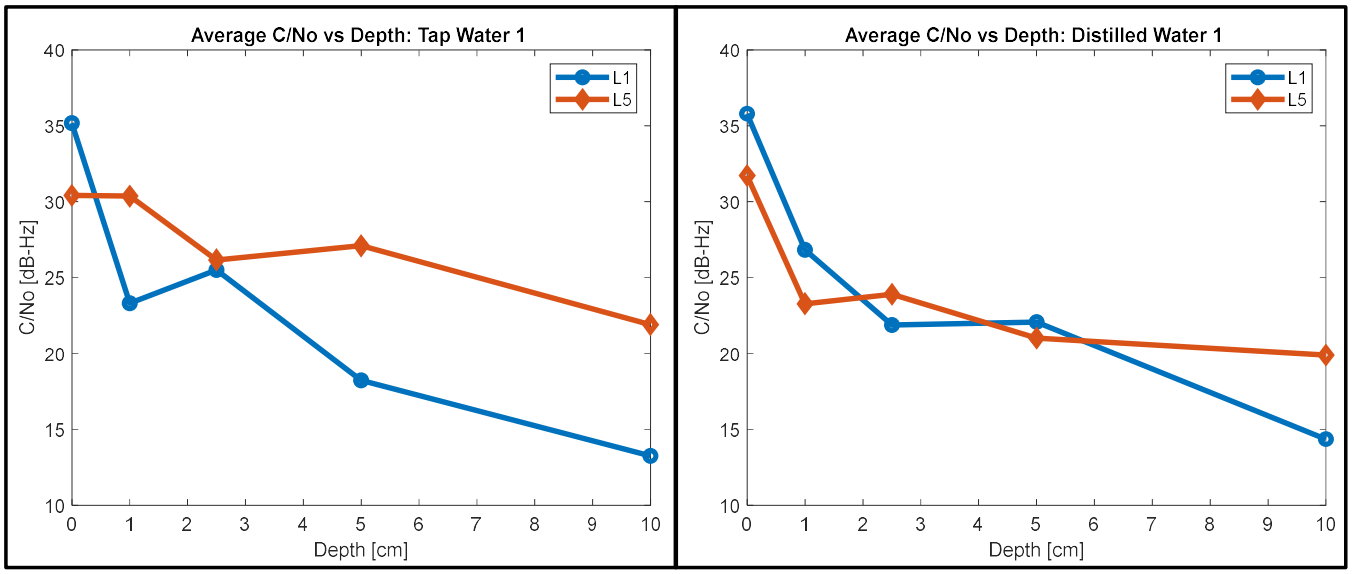

Figure 20. Average C/No vs. Depth of Smartphone under tap (left) and distilled (right) water

Potential Sources of Error

There are many potential contributors to the differences that are seen between our measurements and the theoretical results. On the modeling side, there are several interfaces that were not modeled such as the plastic container, the waterproof bag and perhaps the small amount of air inside the bag. Another unmodeled element is the environment inside the smart phone and its effect on signal reception. As seen already, transmission in water may affect the smartphone antenna efficiency, potentially increasing the relative antenna efficiency of the L5 reception relative to L1. This is source of attenuation due to water that was not modeled. Also, there could be electronics that could interfere or affect the performance. antenna, electronics etc.) Also, there may be some errors from modeling of the medium. For example, we used standard parameters for fresh and salt water which may differ from the actual value of the water used. Another source is due to various simplification we made for the analysis. For example, we used the model for normal incidence angle rather than oblique angle based on the true angle of arrival. Additionally, the analysis was simplified by using depth rather than calculating the propagation distance of each satellite LOS under water for the various depths and times tested. Hence the depths that each signal experienced may be a little different than that used in the modeling which used the vertical depth from the top of water column to the smartphone.

SUMMARY

To maximize the utility of this rapid GNSS positioning technology, we wanted to understand the conditions/depths that GNSS could be received underwater. This could extend the operational window for use of marine GNSS tag for determining positions and allow rapid GNSS positioning technology to even track animals that may only surface for 1-2 seconds at a time. It is also of interest to examine the robustness of GNSS reception in a marine tag should the tag not fully displace water (e.g. if hydrophobic coating over the antenna degrades). We conducted a study of the depth at which GNSS could be received using empirical data and analytical models.

The empirical portion of the study used a smartphone to collect GNSS data. This methodology is useful as we could install software to gather the necessary metrics such as satellites available and signal strength via carrier to noise ratio (C/No) for the analysis. Additionally, we used a smartphone that can receive two GNSS frequencies, L1 (1575.42 MHz) and L5 (1176.45 MHz), to see the effect of frequency on attenuation by water. Different forms of water (distilled, tap and salt water) were tested to examine their effect. Our test results showed that GNSS can reasonably be received under 10 cm of freshwater. In salt water, the attenuation is greater and with reliable reception found at 2.5 cm depth. Of course, this utilized a smartphone and its antenna which generally are not high quality (efficiency) GNSS antennas. With a better antenna, reception depth would improve. These empirical results from freshwater showed more loss than expected based on modeling, particularly on

L1. Finally, we found that L5 performance fared a little better in water than L1 supporting the theory that the smartphone GNSS antenna may not be as efficient on L5 as on L1 due to its electrical length.

ACKNOWLEDGMENTS

The authors thank St. Paul's School Applied Science & Engineering Program.

The views expressed herein are those of the authors only and are not to be construed as official or those of any other person or organization.

REFERENCES

[1] Frank van Diggelen, *A-GPS : assisted GPS, GNSS, and SBAS*, Boston: Artech House, 2009.

[2] Antoine M. Dujon, R. Todd Lindstrom and Graeme C. Hays, "The accuracy of Fastloc-GPS locations and implications for animal tracking," Methods in Ecology and Evolution 2014, 5, 1162–1169, doi: 10.1111/2041-210X.12286

[3] D. P. Costa, P. W. Robinson, P. W., J.P.Y. Arnould, A-L Harrison, S.E. Simmons, et al. 2010. Accuracy of ARGOS Locations of Pinnipeds at-Sea Estimated Using Fastloc GPS. PLoS ONE 5(1): e8677. doi:10.1371/journal.pone.0008677

[4] B. Block, H. Dewar, C. Farwell, ED. Prince, "A new satellite technology for tracking the movements of Atlantic bluefin tuna," Proc. Natl. Acad. Sci. USA Vol. 95, pp. 9384–9389, August 1998;

[5] Gail Schofield, Charles M. Bishop, Grant MacLean, Peter Brown, Martyn Baker, Kostas A. Katselidis, Panayotis Dimopoulos, John D. Pantis, Graeme C. Hays, Novel GPS tracking of sea turtles as a tool for conservation management, Journal of Experimental Marine Biology and Ecology, Volume 347, Issues 1–2, 2007, Pages 58-68, ISSN 0022-0981, https://doi.org/10.1016/j.jembe.2007.03.009.

[6] F. van Diggelen, "Google Analysis Tools for GNSS Raw Measurements, g.co/GNSSTools," Proceedings of the 30th International Technical Meeting of the Satellite Division of The Institute of Navigation (ION GNSS+ 2017), Portland, Oregon, September 2017, pp. 345-356. https://doi.org/10.33012/2017.15172

[7] S. Jiang and S. Georgakopoulos, "Electromagnetic wave propagation into fresh water," Journal of Electromagnetic Analysis and Applications, vol. 3, no. 7, pp. 261-266, 2011

[8] Ghaith Hattab, Mohamed El-Tarhuni, Moutaz Al-Ali, Tarek Joudeh, and Nasser Oaddoumi "An Underwater Wireless Sensor Network with Realistic Radio Frequency Path Loss Model" International Journal of Distributed Sensor Networks, Volume 2013, Article ID 508708, http://dx.doi.org/10.1155/2013/508708

[9] F. Ulaby, R. Moore, and A. Fung, Microwave Remote Sensing: Radar Remote Sensing and Surface Scattering and Emission Theory, Remote Sensing, Addison-Wesley, Reading, Mass, USA, 1981 ~ pg 2022 for v.3

[10] Constantine A. Balanis, "Advanced Engineering Electromagnetics," Second Edition, John Wiley & Sons, Inc., 2012

[11] J.B. Halsted, "Aqueous Dielectric", Chapman and Hall, London, 1973